



Derwent, R. G., Manning, A. J., Simmonds, P. G., Spain, T. G., & O'Doherty, S. (2018). Long-term trends in ozone in baseline and European regionally-polluted air at Mace Head, Ireland over a 30-year period. *Atmospheric Environment*, 179, 279-287.
<https://doi.org/10.1016/j.atmosenv.2018.02.024>

Peer reviewed version

License (if available):
CC BY-NC-ND

Link to published version (if available):
[10.1016/j.atmosenv.2018.02.024](https://doi.org/10.1016/j.atmosenv.2018.02.024)

[Link to publication record in Explore Bristol Research](#)
PDF-document

This is the author accepted manuscript (AAM). The final published version (version of record) is available online via ELSEVIER at <https://www.sciencedirect.com/science/article/pii/S135223101830102X?via%3Dihub> . Please refer to any applicable terms of use of the publisher.

University of Bristol - Explore Bristol Research

General rights

This document is made available in accordance with publisher policies. Please cite only the published version using the reference above. Full terms of use are available:
<http://www.bristol.ac.uk/pure/about/ebr-terms>

1 Long-term trends in ozone in baseline and European regionally-
2 polluted air at Mace Head, Ireland over a 30-year period.

3 Richard G. Derwent^{a,*}, Alistair J. Manning^b, Peter G. Simmonds^c, T. Gerard Spain^d, Simon O'Doherty^c

4 ^a*rdscientific, Newbury, Berkshire RG14 6LH, United Kingdom*

5 ^b*Met Office, FitzRoy Road, Exeter, Devon EX1 3PB, United Kingdom*

6 ^c*School of Chemistry, University of Bristol, Bristol, United Kingdom*

7 ^d*School of Physics, National University of Ireland, Galway, Galway, Ireland*

8

9 *Corresponding author. Tel: +44 1635 41828

10 E-mail address: r.derwent@btopenworld.com (R G Derwent)

11 *Keywords:* surface ozone, trends, baseline levels, Mace Head Ireland, seasonal cycles

12 HIGHLIGHTS

- 13 • 30 years of ozone observations for Mace Head, Ireland are presented
14 • The importance of sorting the observations by air mass is stressed
15 • Northern hemisphere baseline ozone levels have increased, levelled off and begun to decline

16 ABSTRACT

17 Observations of surface ozone, O₃, have been made at the Mace Head Atmospheric Research
18 Station on the North Atlantic Ocean coastline of Ireland over a 30-year period from April 1987
19 through to April 2017. Using meteorological analyses and a sophisticated Lagrangian dispersion
20 model, the hourly observations have been sorted by air mass histories to separate out the
21 observations for northern hemisphere mid-latitude baseline air masses. Monthly average baseline
22 levels showed a pronounced seasonal cycle with spring maxima and summer minima. Baseline levels
23 have shown an increase during the 1980s and 1990s which has been stronger in the winter and
24 spring and weaker in the summer. The rate of this increase has slowed to the extent that baseline
25 levels have been relatively constant through the 2000s and started to decline in 2010s. The unsorted
26 O₃ data has shown different long-term trends from the baseline data because of the influence of
27 European regional NO_x and VOC emissions which have reduced wintertime O₃ levels below the
28 baseline levels and enhanced summertime O₃ levels above them. Episodic peak O₃ levels have

29 declined steadily during the study period but 50 ppb 1-hour exceedances are likely to continue for
30 the foreseeable future.

31

32 **1. Introduction**

33 Tropospheric ozone (O₃) is important both as an oxidant and as a source of hydroxyl (OH) and
34 hydroperoxyl (HO₂) radicals (Levy, 1971). It is widely recognised as an important air pollutant with
35 widespread impacts on human health, crops and vegetation (Monks et al., 2015). O₃ is also a
36 tropospheric greenhouse gas (IPCC, 2007; Stevenson et al., 2013). Because of these impacts, it is the
37 focus of much policy-making activity, the aim of which is to reduce O₃ levels to meet air quality
38 standards and guidelines (WHO, 2006).

39 Much of the understanding that is the bedrock of policy-making has come from O₃ observations and
40 a number of authoritative reviews are available (Vingarazan, 2004; Oltmans et al., 2006; Cooper et
41 al., 2014). Surface O₃ levels over Europe have doubled from the 1950s to around 1990 (Feister and
42 Warmbt, 1987) and in the Swiss Alps the records demonstrate much the same (Staehelin et al.,
43 1994). Ozonesonde data over Europe have shown an increase during the 1980s and 1990s but a
44 decrease in the 2000s (Logan et al., 2012). Studies by Parrish et al., (2012) and Cooper et al., (2010)
45 have demonstrated increases in surface O₃ in spring on the Pacific Ocean coast of the USA. There are
46 preliminary indications of a slowing of this increase and perhaps a reversal of the trend (Parrish et
47 al., 2012; 2014; 2017). Strong increases have been reported for Mount Happono, Japan also during
48 spring (Tanimoto, 2009).

49 An important issue for policy-makers has been the role played by intercontinental O₃ transport and
50 the growth in the hemispheric O₃ background. Regional-scale O₃ episodes are superimposed upon
51 this hemispheric O₃ background and so any rising ozone background may erode the benefits of
52 regional-scale O₃ precursor emission reductions (Jacob, 1999). Decreases in the baseline O₃ entering
53 the USA from across the North Pacific Ocean as monitored at Trinidad Head and Lassen National

54 Park may ease the difficulties faced by policy-makers in achieving air quality standards (Parrish et al.,
55 2017). However, ozone levels monitored at the Mount Bachelor Observatory in Central Oregon
56 appear to be increasing due to global sources and regional wildfire events (Zhang and Jaffe, 2017).
57 Baseline O₃ can be readily monitored in maritime air masses at Mace Head, Ireland, located on the
58 western fringe of Europe, having recently travelled across the North Atlantic Ocean without local
59 influence. Previously, increasing O₃ mixing ratios in baseline air masses have been reported over the
60 period from 1987 to 2003 (Simmonds et al., 2004). This increasing baseline may have partially offset
61 the improvement in European air quality due to O₃ precursor emission reductions (Derwent et al.,
62 2003). More recently, baseline levels have remained roughly constant during the 2000s (Derwent et
63 al., 2013) and have now begun to decline during the 2010s. Here we present a further analysis of the
64 Mace Head O₃ record which has been extended to include 30 years of data from April 1987 onwards.

65 **2. Experimental Methods**

66 Ozone (O₃) measurements were acquired using commercial UV spectrometers and three separate
67 analysers were used over the period of this study. The periods of use were from April 1987 to March
68 2003 (model ML8810, Monitor Labs, San Diego CA), from March 2003 to April 2016 (model 49C,
69 Thermo Electron Inc, Franklin, MA) and from April 2016 to April 2017 (model 49i, Thermo Electron
70 Inc, Franklin, MA). The instruments were operated within the UK Rural Ozone Network, latterly the
71 Automatic Urban/Rural Network (AURN). As part of that network, their calibration was audited 2-4
72 times per year against a National Physical Laboratory-traceable UV photometer transfer standard
73 (Sweeney and Stacey, 1992). The raw voltage output of the Monitor Labs ML8810 was converted to
74 concentration values based on these audits. The Thermo Electron instruments output mixing ratio
75 values directly and have required no adjustments to response factors. Since 1995, the
76 measurements are shared with the national pollution network operated by the Irish Environmental
77 Protection Agency (EPA) who audit the instrument annually against their own NPL-traceable transfer
78 standard. In all cases, the results were found to be within 5% of nominal values. In addition, the

79 instruments (other than the current instrument) have been regularly validated by a system and
80 performance audit (<https://www.empa.ch/web/s503/wcc-empa>) conducted by the World
81 Calibration Centre for surface ozone, (Zellweger et al., 2013) and the performance criteria have
82 consistently been passed as good. These audits are necessarily more rigorous than the more
83 frequent network audits and give a high degree of confidence in the measurements.

84 All analysers operate on a 10 second measurement cycle and data are reported as hourly averages.
85 Prior to 1996, data were recorded as hourly averages. From 1996 onward, data were recorded as
86 one minute averages and, after filtering, averaged to one hour. This permitted a better assessment
87 of instrumental performance and reduced data loss due to short duration events such as filter
88 changes etc. The sampling inlet comprised an inverted PTFE cup to prevent rain ingress, 1/4" PTFE
89 sample tubing and a PTFE filter, 5-um pore size, changed monthly to exclude particulate
90 contamination. The sample inlet was mounted initially at 3m and in March 2005 it was moved to 7m
91 using the same tubing and in December 2014 it was installed at 10m using new tubing. The new
92 tubing had previously been tested and O₃ loss was found to be less than 1ppb. In January 2015, the
93 tubing was sheathed in 1/2" Synflex to exclude light and to ease removal and replacement. At this
94 time, a second, sheathed line was installed at the same height to facilitate instrument inter-
95 comparisons. The filters used were either Pall Zylon P4PH047 (Pall Life Sciences, Ann Arbor, MI) or
96 Millipore Mitex LSWP04700 (Merck Millipore, Carrigtoohil, Co. Cork, Ireland)) both of which were
97 found to produce minimal ozone loss.

98 Central to the analysis and interpretation of the O₃ record at Mace Head, Ireland is the selection of
99 the O₃ measurements in air masses that are representative of the unpolluted Northern Hemispheric
100 marine boundary layer. The O₃ levels in these unpolluted air masses are referred to as baseline levels
101 and, by definition, they should be uninfluenced by local effects or recent regional NO_x emissions
102 from Ireland or Continental Europe. Baseline levels are to be distinguished from background levels
103 which are model constructs describing levels due to natural sources (HTAP, 2010). Over the 30 years

104 of continuous O₃ observations at Mace Head, a number of methods have been developed to assign
105 O₃ mixing ratios to specific air masses (Simmonds et al., 1997), of which two methods have been
106 used here as described previously by Derwent et al., (2013).

107 (1). Pollution filtering. Co-incident measurements of anthropogenic traces such as halocarbons and
108 carbon monoxide are simple but effective indicators of 'polluted' air masses (Cunnold et al., 1986;
109 Simmonds et al., 1993). Halocarbons or carbon monoxide were first flagged as 'polluted' if their
110 values exceeded baselines by 3 standard deviations. To define a pollution event the mixing ratios of
111 at least two other species must show concurrent increases of at least 2 standard deviations, over
112 several consecutive measurement periods. If and only if these two independent species showed
113 simultaneously elevated levels, the values were reported as 'polluted', otherwise the data were
114 reported as 'unpolluted' or baseline, (Cunnold et al., 1986; Simmonds et al., 1993).

115 (2). Lagrangian dispersion modelling. A sophisticated numerical atmospheric dispersion model has
116 been used to indicate air mass histories in terms of 'baseline', 'European', 'southerly', or 'local', as
117 described by Manning et al., (2011). Baseline observations exclude times when the air was modelled
118 to have come significantly from populated regions east of Mace Head (i.e. Ireland, UK and the rest of
119 Europe) or southern latitudes (latitudes less than 35°N), or when the air was not well mixed (i.e. in
120 stable atmospheric conditions). This is our preferred method for sorting air masses but
121 unfortunately it is limited to the period after 1st February 1989 and up to the present date.

122 Because of the presence of the significant levels of O₃ in unpolluted maritime air masses, care had to
123 be taken separating 'polluted' and 'unpolluted' air masses for those months before February 1989
124 when the dispersion model method was not available. With the phase-out of European production
125 and usage of halocarbons and the implementation of vehicle exhaust gas catalysts, the magnitudes
126 of the halocarbon and carbon monoxide peaks from Europe have become smaller with time. As a
127 result, the pollution filtering method has become more inaccurate particularly for ozone and the
128 dispersion model method has become the preferred method for sorting air masses. The 1987 – 2017

129 period has therefore been split into three sections. The section from April 1987 to January 1989,
130 inclusive, utilised the pollution filtering method to sort the ozone data according to whether the air
131 masses were 'polluted' or 'unpolluted'. The section from February 1989 to December 1994 provided
132 a six year overlap period when both methods were operated side-by-side. The section from January
133 1995 to April 2017 utilised the dispersion model method. As detailed in Derwent et al., (2013), a
134 careful analysis of the overlap period indicated that the pollution filtering method gave somewhat
135 lower monthly mean baseline mixing ratios by 1.6 ± 1.9 (1 standard deviation sd) ppb compared with
136 the dispersion model method. This correction was added to the pollution filtering results for the
137 period from 1st April 1987 to 31st January 1989.

138 Over the intervening period since the Lagrangian dispersion modelling sorting method (Manning et
139 al., 2011) has been applied to the Mace Head data, improvements have been made to the sorting
140 algorithm. A population map is now combined with the air history map to infer the total influence of
141 populated regions, including Africa, USA and Eastern Europe on any measurement during each 2-
142 hour period. Additionally, for each 2-hour period, the percentage of model particles leaving the air
143 history domain from the north west (NW) sector (northern Canada and the Arctic regions), southern
144 and upper troposphere edges is estimated. 2-hour periods are defined as being representative of the
145 well-mixed Northern Hemisphere baseline when the overall and land local influences are low (no
146 significant influence from any local emissions), when the influence of European populated regions,
147 Africa, USA and Eastern Europe are all low, and the vast majority of the model particles have left the
148 model domain through the NW sector. With this improved baseline allocation, two or more hours
149 were assigned to the baseline in 317 out of the 339 months between February 1989 and April 2017,
150 leaving 22 months for which the less restricted baseline allocation method of Manning et al., (2011)
151 was employed.

152 A merged baseline dataset was then constructed from the 22 monthly records from the pollution
153 filtering method, 317 monthly records from the improved baseline allocation method employing the

154 Lagrangian dispersion model, back-filled with 22 records from the Manning et al., (2011) method.
155 This merged dataset has been used in the subsequent analyses below and is presented in Figure 1
156 and in electronic form in the Supplementary Information.

157 **3. Ozone levels in Northern Hemisphere baseline air masses**

158 3.1 Baseline trends

159 Using the pollution sorting and dispersion model methods, the O₃ observations have been sorted by
160 air mass origins into distinct and robust categories. We begin with an analysis of the O₃ levels that
161 have been assigned to the baseline category. This category largely excludes air masses that may
162 have been influenced by the highly populated and industrialised regions of Europe, with the majority
163 of the baseline air masses arising from the most northerly regions of North America. With the more
164 restricted allocation methodology employed here within the Lagrangian dispersion model, 11.7% of
165 the available hourly O₃ observations were assigned to the baseline category compared with 36.2%
166 previously with the less restricted allocation methodology (Derwent et al., 2013). The hourly
167 baseline sorted O₃ observations were accumulated up to a monthly basis and the monthly average
168 baseline levels were estimated from whatever baseline allocations were available during that
169 month. Figure 1 presents the complete time series of baseline monthly average O₃ mixing ratios
170 obtained by combining the pollution filtering baseline levels with those from the dispersion model.
171 Visual inspection of the complete time series shows the presence of a well-developed seasonal cycle
172 during each year with a springtime maximum and a summertime minimum, an early period of
173 increasing mixing ratios, a later period of relatively constant mixing ratios and significant year-on-
174 year variability as indicated by the high year in 1999 and the low year in 1987.

175 In most studies of O₃ trends, linear regression is used to fit a straight line through the data to
176 determine the slope of the fit in units of ppb yr⁻¹ (for example: Collette et al., 2016; Cooper et al.,
177 2014; Oltmans et al., 2013). Trends in the annual average baseline O₃ mixing ratios in Figure 1 were
178 analysed and assessed using the Mann-Kendall test (Salmi et al., 2002). The annual averages showed

179 a highly statistically significant (at the 0.01 or 99% level of significance) upwards trend over the 1987
180 – 2017 period. The non-parametric Sen’s method (Salmi et al., 2002) indicated an upwards trend of
181 $+0.22^{+0.10}_{-0.08}$ ppb yr⁻¹ (where the quoted confidence limits here and throughout the study are 95%
182 or 2 – σ confidence limits). In previous studies, we have reported $+0.31 \pm 0.12$ ppb yr⁻¹ (Derwent et
183 al., 2007) and $+0.25 \pm 0.09$ ppb yr⁻¹ (Derwent et al., 2013) for shorter periods, 1987 – 2007 and 1987
184 – 2012, respectively. However, all three linear fits only poorly represented the observations as
185 indicated by the residuals which were negative up to 1995 and after 2010 and were positive
186 between 1998 and 2010. The behaviour of the residuals could be explained if the increase in the
187 baseline had slowed, levelled out and perhaps declined in the later part of the record.

188 To test for any levelling off in the observed trend, a quadratic function of the form:

$$189 \quad Y = a + bt^2 + ct \quad (1).$$

190 was fit through the baseline data where t is the time through the record relative to t = 0 in the year
191 2000. Non-linear regression analysis, (NLREG, Sherrod, 1992), returned a slope (c) of 0.34 ± 0.07 ppb
192 year⁻¹ and an acceleration (or deceleration) term (b) of -0.0225 ± 0.008 ppb year⁻², both of which
193 terms were highly statistically significant at the 95% level of significance. This points to constantly
194 decreasing annual growth rates over the 1987 – 2017 period. The slowing in the annual rate of
195 increase has advanced to the point that annual baseline ozone levels have begun to level off and
196 decrease. The apparent time of maximum, t_{\max} , could be quantified using:

$$197 \quad t_{\max} = -c/(2*b) + 2000 \quad (2).$$

198 Combining the slope and deceleration terms together points to the fitted quadratic function levelling
199 out in 2007 or thereabouts, with a 2 – σ confidence range of ± 6 years. The quadratic fit explained
200 about 80% of the variance in the data whereas the simple linear fit without the acceleration term
201 accounted for about 56%. It is concluded therefore that the baseline Mace Head observations are
202 best explained by the quadratic function, that is to say, by an initially steep rising trend that declines,

203 levels out and ultimately declines during the later years of the record, rather than a simple steady
204 linear trend.

205 The linear fit, ($Y = a + ct$), provides an estimate of the average annual increase in O_3 over the 1989 –
206 2017 data record of $+ 0.27 \pm 0.09$ ppb year⁻¹. The quadratic fit, ($Y = a + bt^2 + ct$), provides an estimate
207 for the average annual rate of change of the O_3 growth rate, indicating a constantly decreasing rate
208 of growth over the 1989 – 2017 data record. It must be noted that neither analysis implies that O_3
209 necessarily varied in a linear or quadratic manner and they do not imply how annual mean O_3 levels
210 will change in the future. They merely provide a convenient way of summarising the observed long-
211 term O_3 changes. Figure 2 presents the annual average baseline O_3 data for 1987 – 2016, together
212 with linear and quadratic fits and their residuals. The superior quality of the quadratic fit is evident,
213 as is the recent decline in ozone levels from 2009 onwards. Inspection of the residuals in Figure 2 for
214 the linear fit showed that the linear fit overestimated the observations at the start and end of the
215 record and underestimated them in the middle. In contrast, the residuals from the quadratic fit were
216 scattered above and below the observations evenly throughout the record.

217 The trend in annual baseline O_3 has not been realised evenly through the months of the year. The
218 trend in the month of January has been different to that in the month of February and so on, as is
219 shown in Table 1, where the quadratic fits have been applied to the Januarys, Februarys and so on.
220 The quadratic fits are highly statistically significant in all months, except for August and October.
221 Also shown in Table 1 are the quadratic fits to the 3-month seasonal averages because the seasonal
222 averaging decreases the confidence limits and thus eases the discussion of statistical significance.
223 Monthly baseline levels showed an initial phase of high growth during the period from 1987 to 1997
224 which was particularly marked during winter and spring months and weaker during the summer
225 months. This initial growth rate has slowed from 1998 onwards. The slowing down of the rate of
226 increase has been most marked during spring and has been least marked in autumn. As a result, the
227 interpolated times of the maxima in the monthly time series using equation (2) have varied from

228 2004 during May and June through to 2017 in August. Spring levels peaked earliest in 2005 whereas
229 autumn levels peaked some six years later in 2011.

230 3.2 Seasonal variations

231 Visual inspection of the time series of monthly baseline average O₃ levels in Figure 1 shows clear
232 evidence of a seasonal cycle with maxima in the months from March through to May and minima in
233 July through to August. Seasonal cycles with springtime maxima are a clear feature of the ozone
234 records at most marine boundary layer stations though the reasons underpinning these maxima
235 have yet to be unambiguously explained (see Monks 2000 and the references therein). Inevitably,
236 different trends in different months of the year may lead to changing seasonal cycles. This has been
237 investigated by Parrish et al., (2013) using eleven mid-latitude data sets including the baseline Mace
238 Head record up to 2012. The conclusion was that there had been an apparent shift in the seasonal
239 cycle at Mace Head but that it was not statistically significant. With the longer baseline record
240 available in this study, we return to the issue of changing seasonal cycles at Mace Head.

241 To accurately characterise the seasonal cycles in the baseline observations, sine curves were fitted
242 through the monthly mean ozone mixing ratios (O₃) using non-linear regression software (NLREG,
243 Sherrod, 1992) which returned five fitted parameters: Y₀, A₁, A₂, φ₁ and φ₂, representing:

$$244 \quad O_3 = Y_0 + A_1 \sin(\chi + \phi_1) + A_2 \sin(2\chi + \phi_2) \quad (1)$$

245 where χ takes the values from 0 to 2π radians in covering one complete year from 1st January to 31st
246 December, Y₀ is the long-term average ozone mixing ratio, A₁ and A₂ are the amplitudes of the
247 fundamental and second harmonics and φ₁ and φ₂ are their phase angles. The 1987 – 2017 baseline
248 record was split into six five-year periods and the average seasonal cycles were calculated for each
249 five-year period and sine curves were fitted through them. The fitted parameters for each five-year
250 period are presented in Table 2.

251 The long-term average value terms (Y_0) clearly show evidence of an increase between 1988 – 1992
252 and 2012 – 2016 which is statistically significant, as would be expected based on section 3.1 above.
253 The amplitudes of the fundamental (A_1) also appear to increase between 1988 – 1992 and 2012 –
254 2016 but by no more than would be expected based on the increase in the Y_0 values. In contrast, the
255 phase angles of the fundamentals (ϕ_1) increased steadily from 1988 – 1992 to 2012 – 2016 by 0.015
256 ± 0.005 radians per year (0.85 ± 0.3 day per year), an increase which was statistically significant. The
257 amplitudes of the second harmonics (A_2) showed a slight downwards trend which was not
258 statistically significant. The phase angles of the second harmonics (ϕ_2) showed no evidence of any
259 significant change throughout the study period.

260 In summary then, it is likely that the differential trends between the different months over the 1987
261 – 2017 period have led to a statistically significant increasing trend of 0.85 ± 0.3 day per year in the
262 phase angle of the fundamental term, $A_1 \sin(\chi + \phi_1)$, of the baseline seasonal cycle, see Table 2.
263 This is equivalent to the maximum in the baseline O_3 seasonal cycle shifting by 0.85 ± 0.3 day per
264 year, or about 8.5 days per decade, earlier in the year as illustrated in Figure 6. This is somewhat
265 larger than the 3.0 ± 3.7 days per decade shift reported by Parrish et al., (2013) which was not
266 statistically significant. The increasing confidence in the shift of the ozone maximum earlier in the
267 year reported here is presumably due to the longer baseline record now available.

268 **4. Analysis of the unsorted Mace Head data**

269 Data repositories (for example: Schultz et al., 2017) and literature reviews (Collette et al., 2016;
270 Cooper et al., 2014; Oltmans et al., 2006) focus on the unsorted Mace Head ozone data because of
271 its widespread availability and ease of access. The unsorted data differs from the baseline data
272 analyses in section 3 above because it includes data for air masses arriving from the continent of
273 Europe, southerly latitudes and those air masses which have been influenced by local ozone sinks. In
274 Figure 3, the monthly average unsorted ozone data are presented, together with the difference
275 between the monthly averages of the baseline data and the unsorted data. Visual inspection of the

276 unsorted data in Figure 2 and the baseline data in Figure 1 reveals many similar features, namely,
277 increasing trends and marked seasonal cycles. The difference plot shows that the unsorted monthly
278 averages are generally lower than the baseline averages and that this difference also shows the
279 presence of trends and marked seasonal cycles.

280 The annual averages of the unsorted O₃ data exhibited similar behaviour over the 1987 – 2017
281 period compared with the baseline data. A linear fit to the unsorted data returned a year 2000 value
282 of 35.6 ± 0.55 ppb and a slope of $+0.17 \pm 0.06$ ppb yr⁻¹ which is significantly smaller than the linear
283 slope found for the baseline data of $+0.27 \pm 0.09$ ppb yr⁻¹. A quadratic fit to the unsorted data
284 returned a year 2000 value of 36.4 ± 0.67 ppb, a linear term of $+0.22 \pm 0.06$ ppb yr⁻¹ and a
285 deceleration term of -0.0123 ± 0.007 ppb yr⁻², implying a turnover during 2008 ± 6 . These fitted
286 parameters are different from the fitted annual baseline parameters reported in Table 1. The
287 differences in the year 2000 values and the deceleration terms were statistically significant at the 2 –
288 σ confidence level but those in the linear terms were only significant at the 1 – σ level. The two sets
289 of annual averages and their quadratic fits are illustrated in Figure 4, showing how different their
290 time series behaviours are on visual inspection. Baseline levels have risen faster than unsorted
291 levels, leading to an increasing divergence between the two datasets with time. There is also a
292 difference in the turn-over behaviour, with a delay in the turnover of the unsorted data which has
293 led to decreasing divergence with time.

294 Visual inspection of the difference plot in Figure 3 shows that the monthly averages of the unsorted
295 mixing ratios were less than the baseline mixing ratios, generating a positive difference (monthly
296 average baseline > unsorted). The differences were largest during the winter months and these
297 wintertime differences appear to have declined during the study period. The differences were most
298 negative (unsorted > baseline) during the summer months and these negative differences also
299 appear to have declined during the study period.

300 Quadratic functions were fitted through the monthly average differences, revealing that the annual
301 average difference increased steadily, then reached a maximum in 2007, before starting to decline,
302 see Table 3. Fitted differences in 2000 were largest in December and least in July. November
303 differences declined steadily, reached a minimum in 2004, before increasing again. In contrast, July
304 differences increased steadily throughout the study period, showing the steepest annual gradient,
305 without any statistically significant evidence of levelling off. Springtime differences rose initially,
306 then levelled off in the early 2000s, before starting to decline towards the end of the record,
307 following the behaviour of the baseline data.

308 Baseline and unsorted O₃ mixing ratios would be closely similar and the (baseline – unsorted)
309 differences would be small, were it not for the O₃ levels found in European regionally polluted air
310 masses arriving at Mace Head and for local influences from the immediate vicinity of the Mace Head
311 Atmospheric Research Station. During winter, European regional NO_x emissions cause depletion of
312 O₃ and so O₃ mixing ratios in the unsorted data drop markedly below baseline levels (Derwent et al.,
313 1998), producing the positive differences evident in Figure 3. During summer, European
314 photochemical O₃ formation from European regional NO_x and VOC emissions drives up O₃ mixing
315 ratios above baseline levels producing the negative differences evident in Figure 3.

316 European NO_x emissions have declined to 48% of their 1990 values by 2015 (European Environment
317 Agency, 2017) and this has reduced the scavenging of O₃ by NO_x, particularly in the winter and in
318 urban areas. Consequently, this has reduced the intensity of NO_x-depletion in the air masses arriving
319 at Mace Head and so decreased the size of the positive differences in Figure 3 with time. Not only
320 have European regional NO_x emissions declined with time but those of VOC emissions have also
321 declined to 51% of their 1990 values by 2015 (European Environment Agency, 2017). This has
322 reduced the intensity of photochemical O₃ formation in polluted air masses arriving at Mace Head
323 (Collette et al., 2016: 2017; Derwent et al., 2013) and so decreased the magnitude of the negative
324 summertime differences in Figure 3 with time.

325 By way of confirmation of the impact that the reductions in European regional NO_x and VOC
326 emissions have had on European regional photochemical O₃ formation, we examine the time series
327 of the number of 50 ppb 1-hour ozone exceedances and the maximum 1-hourly mean O₃ level in
328 each year in Figure 5. The number of 50 ppb exceedances starts at a relatively low level in the 1980s,
329 rises to a maximum in the 2000s and then declines towards the end of the study period. A quadratic
330 fit returned a linear term of $+9.8 \pm 10.2 \text{ yr}^{-1}$ and a deceleration term of $-1.6 \pm 1.0 \text{ yr}^{-2}$, both of which
331 were highly statistically significant, implying a turnover during 2003. This behaviour follows from the
332 increasing spring-time baseline ozone early in the study period and from the decreasing regional
333 scale photochemical ozone formation later in the study period, following on from Figures 3 and 4.

334 In contrast, the maximum 1-hour ozone levels declined steadily throughout the study period, see
335 Figure 5, under the influence of the regional scale ozone precursor emission controls. In this case, a
336 quadratic fit returned a highly statistically significant linear term of $-0.84 \pm 0.48 \text{ ppb yr}^{-1}$ and a
337 deceleration term which was not statistically significant. The fit also returned a year 2000 maximum
338 1-hour mean ozone level of $71 \pm 4 \text{ ppb}$, implying that it will not be until 2025 before maximum 1-
339 hour ozone levels declined to the 50 ppb level, if present trends continue. This 50 ppb metric was
340 selected based on the World Health Organisation air quality guideline of 50 ppb maximum 8-hour O₃
341 concentration (WHO, 2006). However, this analysis is merely illustrative and is intended to illustrate
342 the influence of the European regional NO_x and VOC emission reductions on photochemical O₃
343 formation. It is not an attempt to infer or quantify human health effects. Indeed, the remote nature
344 of the location of the Mace Head Atmospheric Research Station precludes such human health
345 considerations. No policy significance is implied by our selection of the 1-hour averaging time period.

346 **5. Discussion and Conclusions**

347 We have analysed the Mace Head O₃ measurement record with a view to quantifying the changes
348 that have occurred at northern mid-latitudes over the past 30 years. An important aspect of our
349 analysis of the Mace Head O₃ record has been our use of meteorological analyses and a

350 sophisticated Lagrangian dispersion model to sort the hourly observations by air mass histories. In
351 this way, we have assembled a time series of O₃ levels in baseline northern hemisphere mid-latitude
352 air masses which have had minimal influence from continental Europe. The 1987 – 1992 baseline
353 observations revealed a seasonal cycle with a spring maximum and a summer minimum and
354 evidence of an annual trend of +0.37 ppb year⁻¹, (Derwent et al., 1994). The 1987 – 1995 baseline
355 observations exhibited a small increasing trend of +0.19 ppb year⁻¹ (Simmonds et al., 1997). The
356 1987 – 2003 baseline observations showed a trend of +0.49 ppb year⁻¹, with largest trends in the
357 winter and weakest trends in the summer (Simmonds et al., 2004). During the 2000s, baseline O₃
358 levels exhibited evidence of decline and stabilisation, with an average trend of +0.31 ppb year⁻¹ over
359 the 20-year 1987 – 2007 period (Derwent et al., 2007) and +0.25 ppb year⁻¹ over the 25-year period
360 (Derwent et al., 2013). Logan et al., (2012) set the Mace Head baseline observations in the context of
361 European ozone-sondes, measurements on board regular aircraft and alpine mountain-top sites and
362 pointed to O₃ increases from 1987 to 1997, with relatively constant levels since 1999. Parrish et al.,
363 (2012) examined the Mace Head baseline levels together with ten other global O₃ datasets of which
364 five were European in origin, with a view to characterising O₃ changes over several decades. Here,
365 the above assessments of changes in tropospheric O₃ at Mace Head have been extended through to
366 April 2017, thus producing a high quality, 30-year monitoring record.

367 We have been able to demonstrate that the long-term O₃ trends and behaviour are markedly
368 different for the complete unsorted O₃ dataset and that of the baseline O₃ dataset. The differences
369 in the apparent trends between the baseline and unsorted data may seem of academic interest but
370 they do have important policy implications. The linear trend in the unsorted data is about 60% of
371 that found in the baseline data. This becomes an issue when it comes to the evaluation of the
372 performance of the global models in describing the growth in tropospheric O₃ levels since pre-
373 industrial times. Parrish et al., (2014) describe how global models underestimate the growth in
374 tropospheric O₃ since the 1950s and how this is particularly the case for the 1987 – 2012 baseline O₃
375 record at Mace Head. If the unsorted O₃ record had been employed for the Parrish et al., (2014)

376 comparison then the situation would have been viewed much more advantageously for the global
377 models and their inadequacies would have been hidden. However, there is no evidence that the
378 coarse spatial scale global models are able to describe accurately the impact of European regionally-
379 polluted air masses on baseline O₃ levels as revealed in section 4 above and so any apparent
380 agreement between the global models and the unsorted O₃ trends at Mace Head must be
381 coincidental.

382 By way of example, we examine the global model study of Lamarque et al., (2010) which compared
383 the global model trends of +0.17 ppb yr⁻¹ from CAM-Chem and G-PUCCINI with the unsorted Mace
384 Head trend of +0.18 ppb yr⁻¹ because they felt that the unsorted observations were more
385 representative of the global model O₃ fields. However, the global models employed by Lamarque et
386 al., (2010) were too coarse in their spatial resolution (1.9° x 2.5°) and could not accurately represent
387 the regional NO_x-driven ozone sink processes that accounted for the reduction in the trends
388 between the baseline and unsorted datasets. A more rigorous comparison should have been made
389 with the baseline data trend of +0.27 ppb yr⁻¹ and then a large global model underestimation would
390 have been apparent. In a further example, we take the GISS-E2 study of Shindell et al., (2013) in
391 which a comparison was made between their global model trend of +0.04 to +0.17 ppb yr⁻¹ at Mace
392 Head between November 1987 and September 2006 and the observed unsorted trend of +0.18 ppb
393 yr⁻¹, concluding that their model performance was satisfactory. However, a more rigorous
394 comparison should have been made with the much higher baseline trend of +0.27 ppb yr⁻¹ and then
395 the global model would appear to underestimate the observed trend as it has since the 1950s
396 (Parrish et al., 2014).

397 A more straightforward and direct comparison between the Mace Head baseline ozone and global
398 model predictions could be achieved if high time resolution (hourly, say) output were to be made
399 available. The comparison with baseline observations could then be restricted to the conditions
400 when the models themselves predict baseline transport.

401 In previous studies, we have shown how rising baseline O₃ levels may have offset the benefits of
402 European regional O₃ precursor emission controls, particularly in the western fringes of Europe
403 (Derwent et al., 2003). O₃ levels in central Europe may well remain roughly level because the
404 increasing influence of North American and Asian emissions on North Atlantic inflow is
405 counterbalanced by decreasing O₃ production from European regional NO_x and VOC emissions from
406 central Europe itself. It is now clear that the rise in baseline O₃ in air masses entering Europe from
407 across the North Atlantic Ocean has finished and that baseline O₃ levels have now levelled off and
408 begun to decline. As a result, the offsetting and counterbalancing effects should begin to diminish
409 and Europe should begin to see more strongly the benefits of European regional emission reductions
410 on European O₃ air quality. Episodic peak O₃ levels have declined steadily during the study period at
411 Mace Head but 50 ppb 1-hour exceedances are likely to continue for the foreseeable future as the
412 decline in baseline O₃ takes time to work through.

413 **Acknowledgements**

414 We specifically acknowledge the cooperation and efforts of the operators of the Mace Head
415 Atmospheric Research Station and their support staff. We also thank the School of Physics, National
416 University of Ireland, Galway, for making the research facilities at Mace Head, Ireland available. The
417 operation of the Mace Head station was supported by the Climate and Energy: Science and Analysis
418 Division of the Department for Energy and Climate Change UK, under contracts EPG 1/1/130 and
419 142, CPEG 11, 24 and 27, GA 01081, GA 0201 and CESA 002 and also by the National Aeronautic and
420 Space Administration (NASA grants NAGW-732, NAG1-1805, NAG5-3974 and NAG-12099).

421 **References**

422 Collette, A., et al., 2016. Air pollution trends in the EMEP region between 1990 and 2012. EMEP:
423 CCC-Report 1/2016, Norwegian Institute for Air Research, Kjeller, Norway.

424 Collette, A., Solberg, S., Beauchamp, M., Bessagnet, B., Malherbe, L., Guerreiro, C., et al., 2017. Long
425 term air quality trends in Europe – Contribution of meteorological variability, natural factors and
426 emissions. European Topic Centre on Air Pollution and Climate Change Mitigation Technical Paper
427 2016/7, Bilthoven, Netherlands.

428 Cooper, O.R., Parrish, D.D., Stohl, A., Trainer, M., Nedelec, P. Thouret, V., Cammas, J.-P., Oltmans,
429 S.J., Johnson, B.J., Tarasick, D., Leblanc, T., McDermid, I.S., Jaffe, D., Gao, R., Stith, J., Ryerson, T.,
430 Aikin, K., Campos, T., Weinheimer, A., Avery, M.A., 2010. Increasing springtime ozone mixing ratios
431 in the free troposphere over Western North America. *Nature* 463, 344-348,
432 doi:10.1038/nature08708.

433 Cooper, O.R., Parrish, D.D., Ziemke, J., Balashov, N.V., Cupeiro, M., Galbally, I.E., Gilge, S., Horowitz,
434 L., Jensen, N.R., Lamarque, J.-F., Naik, V., Oltmans, S.J., Schwab, J., Shindell, D.T., Thompson, A.M.,
435 Thouret, V., Wang, Y., Zbinden, R.M., 2014. *Elementa: Science of the Anthropocene* 2, 1-28,
436 doi:10.12952/journal.elementa.000029.elementascience.org.

437 Cunnold, D.M., Prinn, R.G., Rasmussen, R.A., Simmonds, P.G., Alyea, F.N., Cardelino, C.A., Crawford, A.J.,
438 Fraser, P.J., Rosen, R.D., 1986. Atmospheric Lifetime and annual release estimates for CFC₃ and CF₂Cl₂
439 from five years of ALE data. *Journal of Geophysical Research*, 91, 10797-10817.

440 Derwent, R.G., Simmonds, P.G., Collins, W.J., 1994. Ozone and carbon monoxide measurements at a
441 remote maritime location, Mace Head, Ireland from 1990-1992. *Atmospheric Environment* **28**, 2623-
442 2637.

443 Derwent, R.G., Simmonds, P.G., Seuring, S., Dimmer, C., 1998. Observations and interpretation of the
444 seasonal cycles in the surface concentrations of ozone and carbon monoxide at Mace Head, Ireland
445 from 1990 to 1994. *Atmospheric Environment* 32, 145-157.

446 Derwent, R.G., Jenkin, M.E., Saunders, S.M., Pilling, M.J., Simmonds, P.G., Passant, N.R., Dollard, G.J.,
447 Dumitrean, P., Kent, A., 2003. Photochemical ozone formation in north west Europe and its control.
448 Atmospheric Environment 37, 1983-1991.

449 Derwent, R.G., Simmonds, P.G., Manning, A.J., Spain, T.G., 2007. Trends over a 20-year period from
450 1987 to 2007 in surface ozone at the atmospheric research station, Mace Head, Ireland.
451 Atmospheric Environment 41, 9091-9098.

452 Derwent, R.G., Manning, A.J., Simmonds, P.G., Spain, T.G., 2013. Analysis and interpretation of 25
453 years of ozone observations at the Mace Head Atmospheric Research Station on the Atlantic Ocean
454 coast of Ireland from 1987 to 2012. Atmospheric Environment 80, 361-368.

455 European Environment Agency, 2017. Air quality in Europe – 2017. EEA Report no. 13/2017,
456 Copenhagen, Denmark.

457 Feister, U., Warmbt, W.G., 1987. Long-term measurements of surface ozone in the German
458 Democratic Republic. Journal of Atmospheric Chemistry 5, 1-21.

459 HTAP (2010). Hemispheric transport of air pollution 2010. Part A.: ozone and particulate matter. Air
460 Pollution Studies No. 17. United Nations, Geneva, Switzerland.

461 IPCC, 2007. Summary for policymakers, in: Climate Change 2007: The Physical Science Basis.
462 Cambridge University Press, Cambridge, UK.

463 Jacob, D.J., Logan, J.A., Murti, P.P., 1999. Effect of rising Asian emissions on surface ozone in the
464 United States. Geophysical Research Letters 26, 2175-2178.

465 Lamarque, J.-F., Bond, T.C., Eyring, V., Granier, C., Heil, A., Zlimont, Z., Lee, D., Liousse, C., Mieville,
466 A., Owen, B., Schultz, M.G., Shindell, D., Smith, S.J., Stehfest, E., Van Ardenne, J., Cooper, O.R.,
467 Kainuma, M., Mahowald, N., McConnell, J.R., Naik, V., Riahi, K., van Vuuren, D.P., 2010. Historical
468 (1850 – 2000) gridded anthropogenic and biomass burning emissions of reactive gases and aerosols:
469 methodology and application. Atmospheric Chemistry and Physics 10, 7017-7039.

470 Levy, H., 1971. Normal atmosphere: large radical and formaldehyde concentrations predicted.
471 Science 173, 141-143.

472 Logan, J.A., Staehelin, J., Megretskaja, I.A., Cammas, J.-P., Thouret, V., Claude, H., De Backer, H.,
473 Steinbacher, M., Scheel, H.-E., Stubi, R., Frohlich, M., Derwent, R., 2012. Changes in ozone over
474 Europe: Analysis of ozone measurements from sondes, regular aircraft (MOZAIC) and alpine surface
475 sites. Journal of Geophysical Research 117, D09301, doi:10.1029/2011JD016952.

476 Manning, A.J., O'Doherty, S., Jones, A.R., Simmonds, P.G., Derwent, R.G., 2011. Estimating UK
477 methane and nitrous oxide emissions from 1990 to 2007 using an inversion modelling approach.
478 Journal of Geophysical Research 116, D02305, doi:10.1029/2010JD014763.

479 Monks, P.S., 2000. A review of the observations and origins of the spring ozone maximum.
480 Atmospheric Environment 34, 3545-3561.

481 Monks, P.S., Archibald, A.T., Colette, A., Cooper, O., Coyle, M., Derwent, R., Fowler, D., Granier, C.,
482 Law, K.S., Mills, G.E., Stevenson, D.S., Tarasova, O., Thouret, V., von Schneidmesser, E., Sommariva,
483 R., Wild, O., Williams, M.L., 2015. Tropospheric ozone and its precursors from the urban to the
484 global scale from air quality to short-lived climate forcer. Atmospheric Chemistry and Physics 15,
485 8889-8973.

486 Oltmans, S., Lefohn, A.S., Harris, J.M., Galbally, I.E., Scheel, H.E., Bodekerf, G., Brunke, E., Claude, H.,
487 Tarasick, D., Johnson, B.J., Simmonds, P.G., Shadwick, D., Anlauf, K., Hayden, K., Schmidlin, F.,
488 Fujimoto, T., Akagi, K., Meyer, C., Nichol, S., Davies, J., Redonda, A., Cuevas, E., 2006. Long-term
489 changes in tropospheric ozone. Atmospheric Environment 40, 3156-3173.

490 Oltmans, S.J., et al., 2013. Recent tropospheric ozone changes – A pattern dominated by slow or no
491 growth. Atmospheric Environment 67, 331-351.

492 Parrish, D.D., Law, K.S., Staehelin, J., Derwent, R., Cooper, O.R., Tanimoto, H., Volz-Thomas, A., Gilge,
493 S., Scheel, H.-E., Steinbacher, M., Chan, E., 2012. Long-term changes in lower tropospheric baseline

494 ozone concentrations at northern mid-latitudes. *Atmospheric Chemistry and Physics* 12, 11,485-
495 11,504.

496 Parrish, D.D., Law, K.S., Staehelin, J., Derwent, R., Cooper, O.R., Tanimoto, H., Volz-Thomas, A., Gilge,
497 S., Scheel, H.-E., Steinbacher, M., Chan, E., 2013. Lower tropospheric ozone at northern midlatitudes:
498 changing seasonal cycle. *Geophysical Research Letters* 40, 1631-1636.

499 Parrish, D.D., Lamarque, J.-F., Naik, V., Horowitz, L., Shindell, D.T., Staehelin, J. Derwent, R., Cooper,
500 O.R., Tanimoto, H., Volz-Thomas, A., Gilge, S., Scheel, H.-E., Steinbacher, M., Frohlich, M., 2014.
501 Long-term changes in lower tropospheric baseline ozone concentrations: Comparing chemistry-
502 climate models and observations at northern latitudes. *Journal of Geophysical Research* 119, 5719-
503 5736, doi:10.1002/2013JD021435.

504 Parrish, D.D., Cooper, O.R., Petropavlovskikh, I., Oltmans, S.J., 2017. Reversal of long-term trend in
505 baseline ozone concentrations at the North American west coast. *Geophysical Research Letters* 44,
506 10675-10681.

507 Salmi, T., Maata, A., Antilla, P., Ruoho-Airola, T., Amnell, T. 2002. Detecting trends of annual values
508 of atmospheric pollutants by the Mann-Kendall test and Sen's slope estimates – The Excel template
509 application Makesens. Finnish Meteorological Institute, Helsinki, Finland.

510 Schultz, M.G., Schroeder, S., Lyapina, O, Cooper, O.R., 2017. Tropospheric Ozone Assessment Report:
511 Database and metrics of global surface ozone observations. *Elementa: Science of the Anthropocene*
512 5, doi:http://doi.org/10.1525/elementa.244.

513 Sherrod, 1992. NLREG software.

514 Shindell, D.T., Pechovy, O., Voulgarakis, A., Faluvegi, G., Nazarenko, L., Lamarque, J.-F., Bowman, K.,
515 Milly, G., Kovari, B., Ruedy, R., Schmidt, G.A., 2013. Interactive ozone and methane chemistry in
516 GISS-E2 historical and future climate simulations. *Atmospheric Chemistry and Physics* 13, 2653-2689.

517 Simmonds, P.G., Cunnold, D.M., Dollard, G.J., Davies, T.J., McCulloch, A., Derwent, R.G., 1993. Evidence
518 for the phase-out of CFC use in Europe over the period 1987-1990. *Atmospheric Environment* 27A 1397-
519 1407.

520 Simmonds, P.G., Seuring, S., Nickless, G., Derwent, R.G., 1997. Segregation and interpretation of ozone
521 and carbon monoxide measurements by air mass origin at the TOR station Mace Head, Ireland from
522 1987 to 1995. *Journal of Atmospheric Chemistry* 28, 45-49.

523 Simmonds, P.G., Derwent, R.G., Manning, A.J., Spain, T.G., 2004. Significant growth in surface ozone
524 at Mace Head, Ireland 1987-2003. *Atmospheric Environment* 38,4769-4778.

525 Staehelin, J., Thudium, J., Buehler, R., Volz-Thomas, A., Graber, W., 1994. Trends in surface ozone
526 concentrations at Arosa (Switzerland). *Atmospheric Environment* 28, 75-87.

527 Stevenson, D.S., Young, P. J., Naik, V., Lamarque, J.-F., Shindell, D.T., Voulgarakis, A., Skeie, R. B.,
528 Dalsoren, S. B., Myhre, G., Berntsen, T. K., Folberth, G. A., Rumbold, S. T., Collins, W. J., MacKenzie, I.
529 A., Doherty, R. M., Zeng, G., van Noije, T. P. C., Strunk, A., Bergmann, D., Cameron-Smith, D.,
530 Plummer, D.A., Strode, S. A., Horowitz, L., Lee, Y. H., S., Sudo, K., Nagashima, T., Josse, B., Cionni, I.,
531 Righi, M., Eyring, V., Conley, A., Bowman, K. W., Wild, O., Archibald, A., 2013. Tropospheric ozone
532 changes, radiative forcing and attribution to emissions in the Atmospheric Chemistry and Climate
533 Model Intercomparison Project (ACCMIP). *Atmospheric Chemistry and Physics* 13, 3063-3085.

534 Sweeney, B., Stacey, B., 1992. Intercomparison and intercalibration techniques employed for the
535 U.K. National air monitoring networks. Warren Spring Laboratory Report, Stevenage, U.K.

536 Tanimoto, H., 2009. Increase in springtime tropospheric ozone at a mountainous site in Japan for the
537 period 1998 – 2006. *Atmospheric Environment* 43, 1358-1363.

538 Vingarazan, R., 2004. A review of surface ozone background levels and trends. *Atmospheric*
539 *Environment* 38, 3431-3442.

540 WHO, 2006. Air quality guidelines. Global update 2005. The Regional Office for Europe of the World
541 Health Organization, Copenhagen, Denmark.

542 Zellweger, Klausen, J., Buchmann, B., 2005. System and performance audit for surface ozone, carbon
543 monoxide and methane. Global GAW Station Mace Head Ireland May 2005. EMPA Report 05/2,
544 WMO World Calibration Centre for Surface Ozone, Carbon Monoxide and Methane, Dubendorf,
545 Switzerland.

546 Zhang, L., Jaffe, D.A., 2017. Trends and sources of ozone and sub-micron aerosols at the Mt.
547 Bachelor Observatory (MBO) during 2004-2015. Atmospheric Environment 165, 143-154.

548

549

550 Table 1. Linear, c, and deceleration coefficients, b, obtained by fitting quadratic functions of the
 551 form: $Y = a + bt^2 + ct$, through the monthly baseline average ozone levels at Mace Head, Ireland over
 552 the period from April 1987 to April 2017.

Month	Linear coefficient, ppb year ⁻¹	Deceleration coefficient, ppb year ⁻²	Year 2000 value, ppb	Interpolated year of maximum ^b
-------	--	--	----------------------	---

553

January	+0.40 ± 0.09	-0.0215 ± 0.010	41.65 ± 1.0	2009 ± 5
February	+0.46 ± 0.15	-0.0234 ± 0.016	42.91 ± 1.6	2009 ± 7
March	+0.33 ± 0.11	-0.0227 ± 0.012	45.84 ± 1.2	2007 ± 7
April	+0.42 ± 0.13	-0.0311 ± 0.015	47.53 ± 1.6	2006 ± 4
May	+0.28 ± 0.16	-0.0342 ± 0.020	45.96 ± 1.9	2004 ± 1
June	+0.29 ± 0.12	-0.0302 ± 0.015	38.31 ± 1.5	2004 ± 3
July	+0.32 ± 0.11	-0.0167 ± 0.014	31.80 ± 1.4	2009 ± 8
August	+0.29 ± 0.14	-0.0083 ± 0.017 ^a	31.97 ± 1.7	2017 ± 19
September	+0.22 ± 0.14	-0.0127 ± 0.017	35.82 ± 1.7	2008 ± 6
October	+0.26 ± 0.14	-0.0087 ± 0.017 ^a	37.62 ± 1.7	2015 ± 16
November	+0.34 ± 0.15	-0.0152 ± 0.018	40.06 ± 1.8	2011 ± 14
December	+0.32 ± 0.09	-0.0114 ± 0.010	40.34 ± 1.0	2014 ± 7
Winter (DJF)	+0.39 ± 0.08	-0.0218 ± 0.010	41.78 ± 0.9	2009 ± 4
Spring (MAM)	+0.30 ± 0.10	-0.0272 ± 0.012	46.44 ± 1.1	2005 ± 2
Summer (JJA)	+0.30 ± 0.10	-0.0184 ± 0.012	34.03 ± 1.2	2008 ± 6
Autumn (SON)	+0.28 ± 0.09	-0.0124 ± 0.011	37.83 ± 1.1	2011 ± 11
Annual	+0.34 ± 0.07	-0.0225 ± 0.008	40.10 ± 0.8	2007 ± 6

554

555 ^a Not considered significantly different from zero.

556 ^bFor an explanation of the interpolated year of maximum, see text

557 Table 2. Fitted parameters (Y_0 , A_1 , A_2 , ϕ_1 , ϕ_2) quantifying the seasonal cycles in baseline ozone over
 558 five-year periods at Mace Head, Ireland.

Period	Y_0 , ppb	A_1 , ppb	A_2 , ppb	ϕ_1 , radians	ϕ_2 , radians
1988 - 1992	35.5 ± 0.8	3.7 ± 1.1	4.0 ± 1.1	0.37 ± 0.30	-2.38 ± 0.27
1993 - 1997	36.7 ± 0.9	6.2 ± 1.2	2.3 ± 1.2	0.41 ± 0.20	-2.43 ± 0.52
1998 - 2002	41.2 ± 0.7	6.5 ± 1.0	3.2 ± 1.0	0.47 ± 0.16	-2.44 ± 0.32
2003 - 2007	40.7 ± 0.7	5.7 ± 1.0	3.6 ± 1.0	0.61 ± 0.17	-2.49 ± 0.27
2008 - 2012	40.9 ± 0.6	6.1 ± 0.9	3.8 ± 0.9	0.57 ± 0.15	-2.40 ± 0.23
2012 - 2016	40.7 ± 0.5	5.2 ± 0.8	2.2 ± 0.8	0.74 ± 0.15	-2.41 ± 0.35
1988 - 2016	39.2 ± 0.5	5.5 ± 0.7	3.1 ± 0.7	0.51 ± 0.13	-2.40 ± 0.23
Trend @ 2000	40.0 ± 0.6	6.1 ± 0.8	3.3 ± 0.8	0.43 ± 0.13	-2.45 ± 0.24

560

561

562 Table 3. Linear, c, and deceleration coefficients, b, obtained by fitting quadratic functions of the
 563 form: $Y = a + bt^2 + ct$, through the monthly excess baseline mixing ratios over unsorted mixing ratios
 564 at Mace Head, Ireland over the period from April 1987 to April 2017.

Month	Linear coefficient, ppb year ⁻¹	Deceleration coefficient, ppb year ⁻²	Year 2000 value, ppb	Interpolated year of maximum
-------	--	--	----------------------	------------------------------

565

January	+0.063 ± 0.18 ^a	-0.018 ± 0.020	6.5 ± 1.9	2002 ± 5
February	+0.160 ± 0.14	-0.011 ± 0.016	4.6 ± 1.6	2007 ± 12
March	+0.079 ± 0.11	-0.004 ± 0.012 ^a	4.1 ± 1.2	b
April	+0.073 ± 0.08	-0.008 ± 0.010	3.4 ± 1.0	2005 ± 8
May	+0.096 ± 0.15	-0.015 ± 0.018	3.3 ± 1.8	2003 ± 6
June	+0.107 ± 0.14	-0.002 ± 0.016 ^a	1.5 ± 1.6	b
July	+0.182 ± 0.12	-0.002 ± 0.014 ^a	0.6 ± 1.4 ^a	b
August	+0.125 ± 0.12	-0.000 ± 0.014 ^a	0.9 ± 1.4	b
September	+0.101 ± 0.09	-0.004 ± 0.012 ^a	2.3 ± 1.2	b
October	+0.004 ± 0.13 ^a	-0.006 ± 0.016 ^a	3.6 ± 1.6	b
November	-0.090 ± 0.10	0.010 ± 0.012	4.1 ± 1.2	2004 ± 7
December	-0.103 ± 0.15	-0.009 ± 0.018	7.1 ± 1.8	b
Annual	+0.069 ± 0.07	-0.005 ± 0.038	3.5 ± 0.4	2007 ± 7

566

567 ^a Not considered significantly different from zero at the 1 – σ level of confidence.

568 b: no statistically significant levelling off.

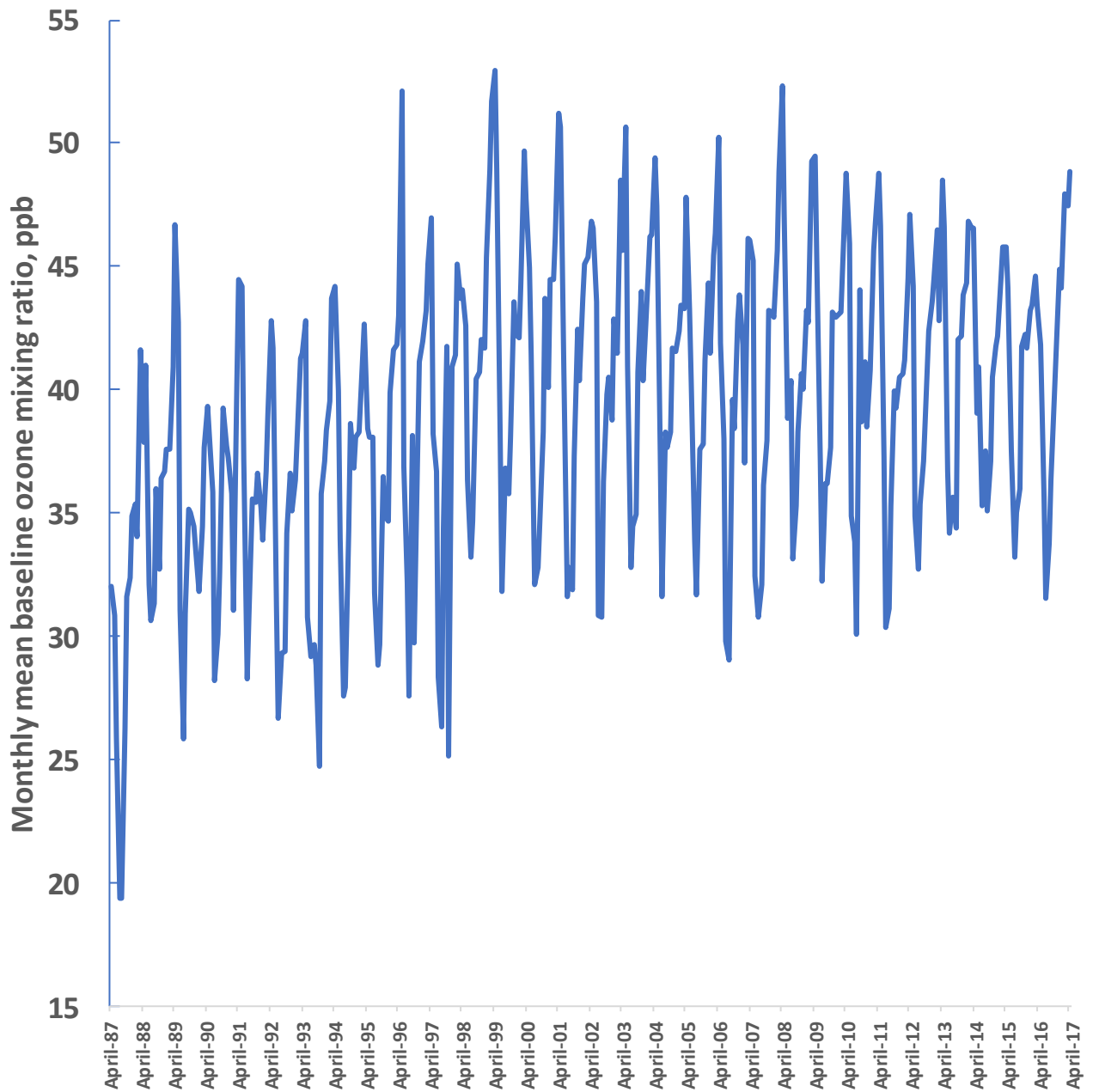
569

570

571

572

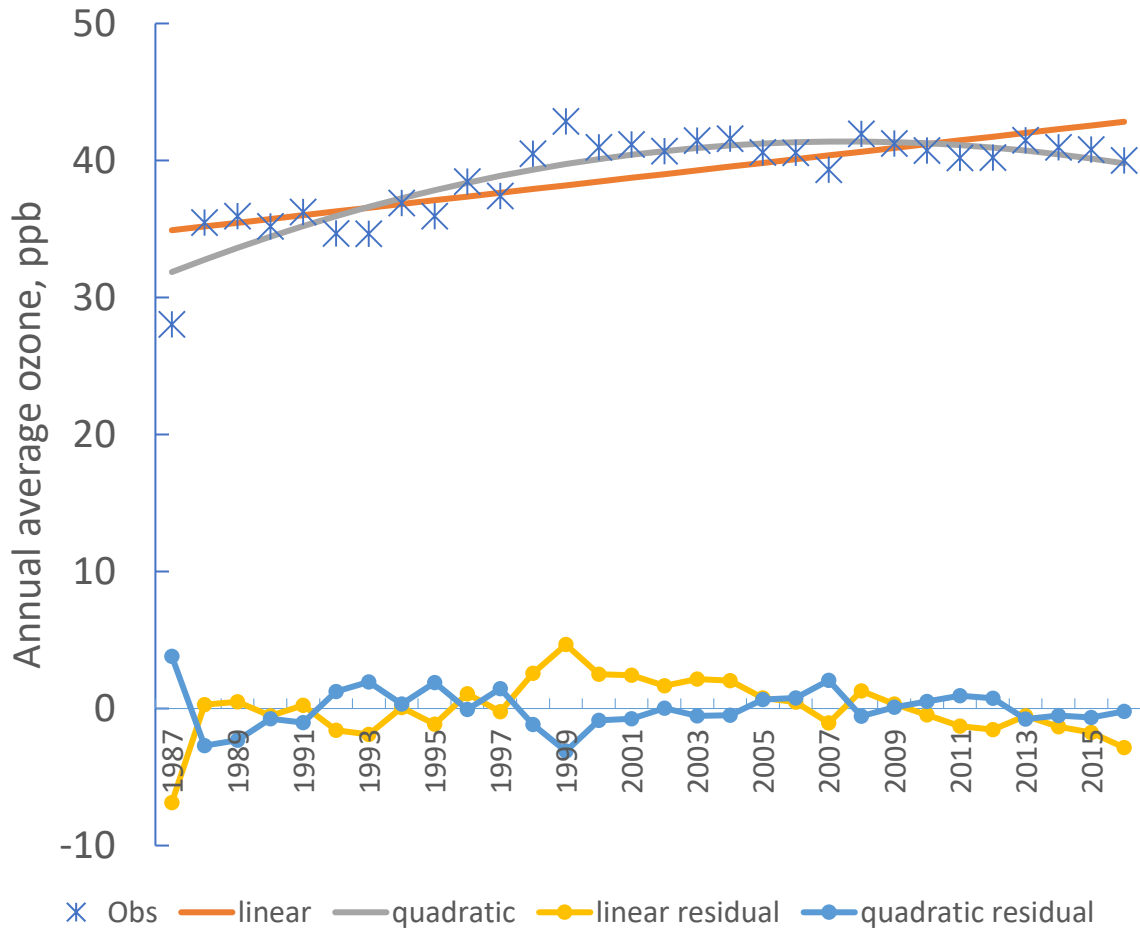
573



574

575 Figure 1. Baseline monthly average O₃ mixing ratios at the Mace Head Atmospheric Research Station
 576 over the period from April 1987 to April 2017.

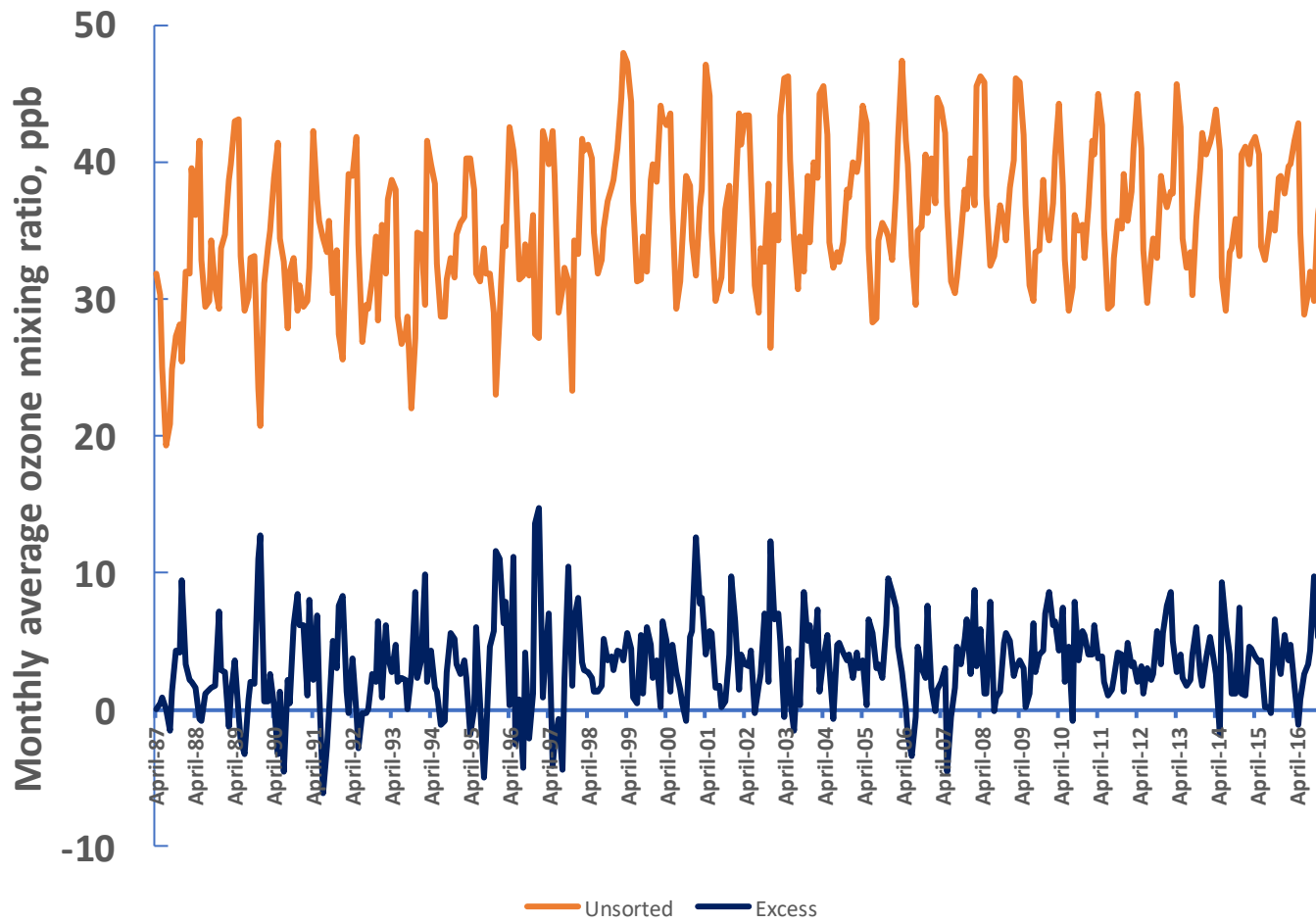
577



578

579 Figure 2. Annual average baseline O₃ data for 1987 – 2016, together with linear and quadratic fits
 580 and their residuals.

581



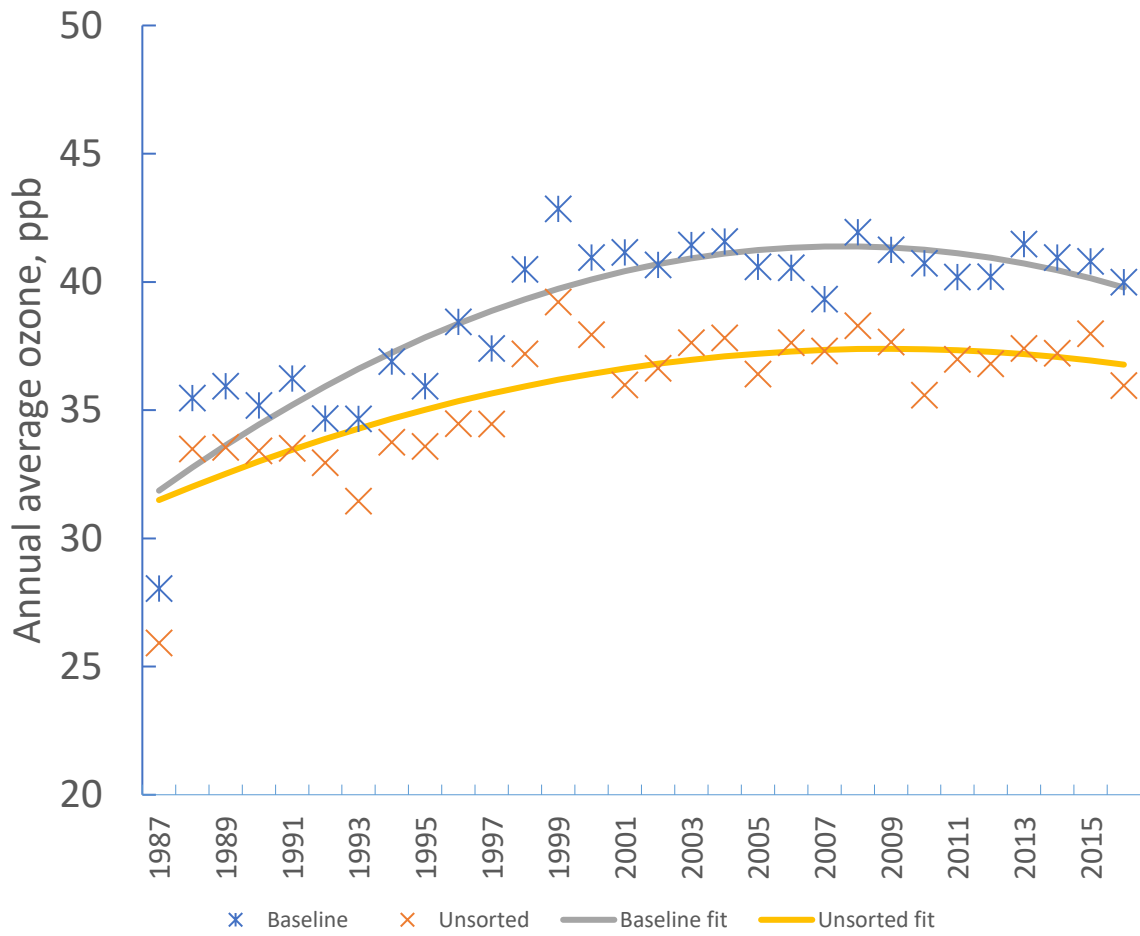
582

583

584 Figure 3. Monthly average unsorted ozone mixing ratios and their differences from the baseline
 585 monthly average O₃ mixing ratios at the Mace Head Atmospheric Research Station over the period
 586 from April 1987 to April 2017.

587

588

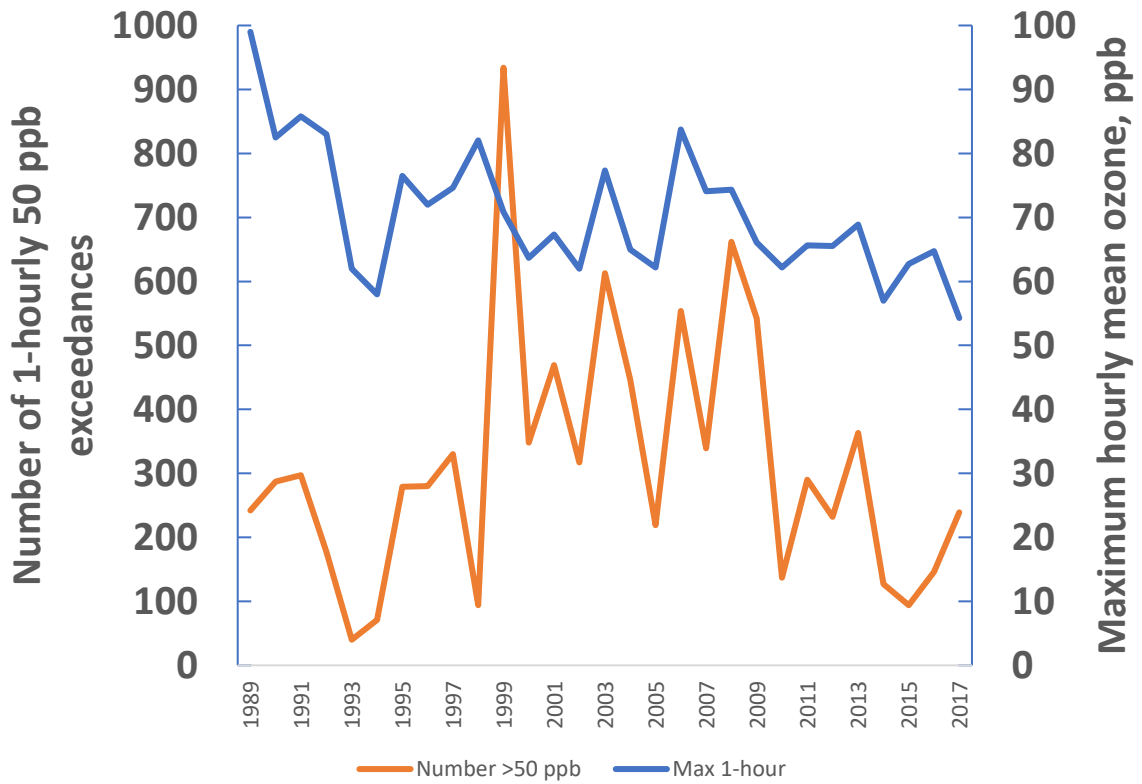


589

590 Figure 4. Annual average baseline and unsorted O₃ data for 1987 – 2016, together with quadratic
591 fits.

592

593

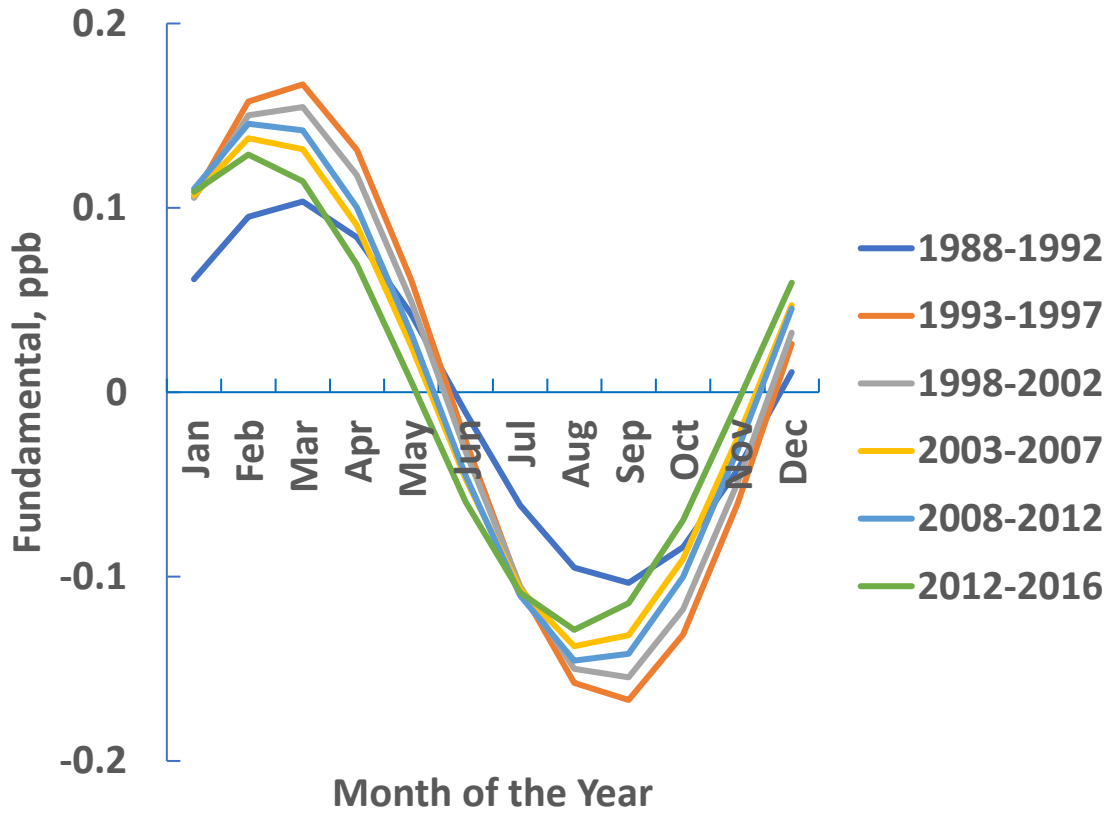


594

595 Figure 5. Number of 1-hourly ozone levels above 50 ppb and the maximum 1-hourly mean ozone
 596 level in each year between 1987 and 2017 at Mace Head, Ireland.

597

598



599

600 Figure 6. Fundamental terms of the seasonal cycles in baseline ozone for the five-year periods 1988-
 601 1992, 1993-1997, 1998-2002, 2003-2007, 2008-2012, 2012-2016.